High-Power Raman Soliton Generation at 1.7 µm in All-Fiber Polarization-Maintaining Erbium-Doped Amplifier

Zi-Peng Xu(徐子鹏), Xuan Wang(王萱), Chuan-Fei Yao(姚传飞)*, Lin-Jing Yang(杨林京), and Ping-Xue Li(李平雪)*

Institute of Ultrashort Pulsed Laser and Application, Beijing University of Technology, Beijing 100124, China

(Received 23 February 2024; accepted manuscript online 23 April 2024)

An all-fiber polarization maintaining high-power laser system operating at 1.7 µm based on the Raman-induced soliton self-frequency shifting effect is demonstrated. The entirely fiberized system is built by erbium-doped oscillator and two-stage amplifiers with polarization maintaining commercial silica fibers and devices, which can provide robust and stable soliton generation. High-power soliton laser with the average power of 0.28 W, the repetition rate of 42.7 MHz, and pulse duration of 515 fs is generated directly from the main amplifier. Our experiment provides a feasible method for high-power all-fiber polarization maintaining femtosecond laser generation working at 1.7 µm.

DOI: 10.1088/0256-307X/41/5/054201

Ultrashort pulse fiber lasers exhibiting ultra short time scale and high peak power have attracted a great deal of attention in many fields including optical communication, material processing, biomedicine, security, and scientific research. In recent years, multiphoton microscopy (MPM) using femtosecond laser sources has become a valuable tool for biological and medical imaging.[1–7] MPM is a nonlinear optical imaging technique that is especially useful for non-invasive three-dimensional imaging deep within scattered biological tissues. The femtosecond laser source wavelength selection of MPM is crucial for improving the depth of multiphoton imaging. Both the 1.3 µm and 1.7 µm excitation windows which have smaller water-absorption than others have been demonstrated to be suitable for deep-tissue imaging in both brain and skin samples *in vivo*.[8] In addition, because shifting the wavelength to longer excitation windows can effectively reduce tissue scattering, the excitation wavelength at the 1.7 µm excitation window has even smaller attenuation compared with the 1.3 µm window. Therefore, ultrashort pulse fiber lasers working at 1.7 µm wavelength become a high-quality light source using for MPM. However, due to the wavelength of 1.7 µm falls into the spectral gap between Er^{3+} and Tm^{3+} emissions, the development of high-power femtosecond fiber laser sources working at 1.7 µm remains a challenge.

The thulium-doped fiber (TDF) laser is a solution to obtain the high-power 1.7 µm ultrashort pulse light source. In 2022, Chen *et al.* demonstrated a dissipative soliton seeded TDF chirped pulse amplification (CPA) system at 1.7 µm waveband. The output power of system is 1.3 W with 348 fs pulse width.[9] However, to realize the short-wavelength operation of the TDF laser, short length of active fiber and high excitation densities need to be used to reduce the reabsorption in TDF, which result in significant power loss. In addition, the pulse compressor in the CPA system is a pair of spatial structured transmission gratings, resulting in the system to be not entirely fiberized.

The other popular technique to obtain ultrashort pulses at 1.7 µm is Raman soliton lasers taking advantage of the soliton self-frequency shift (SSFS).[10–19] When propagating in optical fibers, soliton pulses are affected by stimulated Raman scattering (SRS), causing energy to continuously transfer from the shorter wavelength to the longer wavelength, resulting in SSFS. In fact, the current method to obtain the 1.7 µm high-power femtosecond fiber laser using for MPM is through SSFS in large-mode-area (LMA) passive fiber.[10–13] However, the connection between the LMA passive fiber and pump sources in the laser system is achieved through spatial docking, which requires regular optical path adjustment and dust removal maintenance, resulting in low long-term stability and poor environmental adaptability of the laser system. To improving the robust and integration of system, the entirely fiberized high-power ultrashort pulse lasers without spatial structure modules have become an important research focus.[20–23] In recent years, some solutions for generating 1.7 µm Raman solitons with all-fiber structure have been reported.[14–19] Unfortunately, most of them have not achieved 1.7 µm Raman soliton outputs with an average power exceeding 100 mW.[14–18] In 2016, Nicholson *et al.* demonstrated an all-fiber Raman soliton laser working at 1672 nm with average output power of 1.1 W based on a polarization-maintaining, very-large-mode area (VLMA), erbium-doped fiber.[19] However, the VLMA erbium-doped fiber is not commercially available yet. Therefore, while some progress has been made in this field, it is still necessary to explore a high-power all-fiber femtosecond laser source working at 1.7 µm.

*Corresponding authors. Email: pxli@bjut.edu.cn; yaochuanfei@bjut.edu.cn
© 2024 Chinese Physical Society and IOP Publishing Ltd

In this work, we demonstrate a high-power all-fiber polarization maintaining (PM) femtosecond laser system of 1.7 µm wavelength based on the Raman-induced SSFS in an erbium-doped amplifier. By optimizing the ultra-short pulse based on nonlinear compression generated from pre-amplification stage, the system realizes Raman-induced SSFS in the main amplifier, which can deliver Raman solitons output with the average power of 283 mW, the repetition rate of 42.7 MHz, and the pulse duration of 515 fs. The system consists of commercial silica fibers and devices, which can be easily implemented in photonics laboratory.

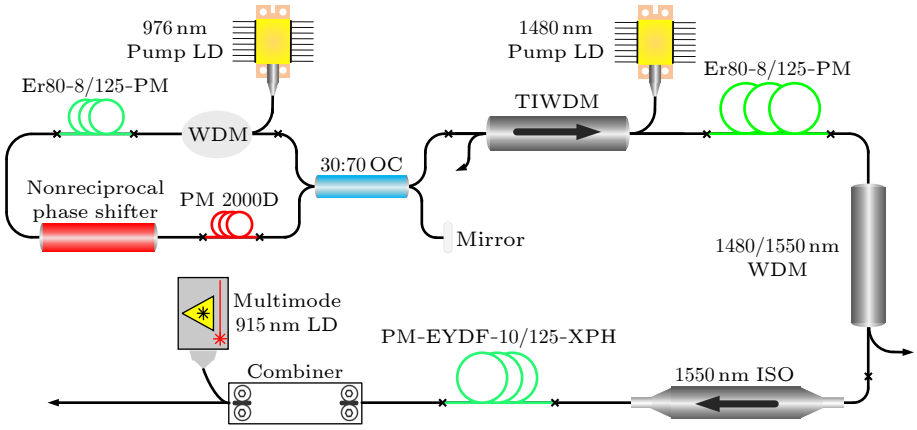

Fig. 1. Experimental setup of Raman soliton generation. WDM: wavelength division multiplexing, LD: laser diode, OC: output coupler, TIWDM: tap + isolator + WDM hybrid, ISO: isolator.

The experimental setup diagram of the system device for generating high-power 1.7 µm Raman soliton is shown in Fig. 1. The entirely fiberized system is composed of PM fiber-pigtailed components and PM fibers, except for the pump light sources. The seed laser of system is an all-fiber oscillator which utilizes the nonlinear amplified loop mirror (NALM) mechanism to achieve mode locking. The PM oscillator is constructed by a 2×2 PM fiber coupler with the splitting ratio of 30 : 70, a 976/1550 nm PM wavelength-division multiplexer (WDM), a 49-cm-long erbium-doped PM single-mode fiber (SMF) (Liekki Er80-8/125-PM) with negative group velocity dispersion (GVD) of $-21.5\,\mathrm{ps}^2/\mathrm{km}$ at 1560 nm, a PM nonreciprocal phase shifter with $\pi/2$ linear phase bias, a 65-cm-long PM dispersion compensating fiber (DCF) (Nufern PM2000D) inducing approximately $0.048\,\mathrm{ps}^2$ group delay dispersion (GDD), and a PM fiber mirror. Two arms on one side of the 2×2 PM fiber coupler are ringed up to form the NALM loop, where the WDM, the erbium-doped PM SMF, the PM phase shifter, and the PM DCF are sequentially fuse-spliced together. One fiber arm on the other side of the 2×2 PM fiber coupler is connected with a PM fiber mirror; the other fiber arm is taken for output port of the oscillator. A single-mode 976 nm pump laser diode (LD) with maximum power of 300 mW is connected through the WDM. The total cavity length of the PM mode-locked oscillator based on NALM is about 4.3 m with net group delay GDD of approximately $-0.032\,\mathrm{ps}^2$ at 1560 nm. Next, the pulses from the seed laser are sent to the two PM cascaded fiber power amplifiers. The first power amplifier named pre-amplification stage consists of a 2.1-m-long PM erbium-doped active fiber as the same as the gain fiber in the PM fiber oscillator pumped by a single-mode 1480 nm LD with maximum power of 800 mW. A 1480/1550 nm PM WDM is placed after pre-amplification stage to remove the unabsorbed 1480 nm pump light by using the common port of the WDM to connect the output port of pre-amplification stage. The output pulses from signal port of 1480/1550 nm WDM is delivered into the second power amplifier called the main amplifier, which is employed to act as both the Raman shifter and the amplifier in the system. The two amplifiers are separated with isolators to avoid parasitic back reflections.

The main amplifier is based on a 1.9-m-long PM erbium/ytterbium-doped double clad (DC) fiber (Nufern PM-EYDF-10/125-XPH) with 10 µm core and 125 µm cladding diameter. The PM active fiber is backward cladding pumped by a multimode 915 nm LD with available power of 25 W through a PM signal-pump combiner. The fiber of the signal port of the combiner is PM-GDF-1550, which is a PM passive DC fiber allowing for low splice loss to erbium/ytterbium-doped DC fibers and standard single-mode PM fiber. The gain fiber and combiner are placed on a water-cooled copper plate. The output port of the combiner pigtail is angle cleaved to avoid back reflections. All components of the system have silica fiber pigtails and can be connected by fusion.

The spectral and temporal characteristics of the output pulses from the oscillator and the pre-amplification stage were obtained by using a Yokogawa AQ6370D optical spectrum analyzer, a Femtochrome FR-103 XL autocorrelator, and a RIGOL DS2202A oscillometer with a Newport 818-BB-51F biased detector. The measured experimental results are shown in Figs. 2 and 3. The PM fiber oscillator can achieve self-started mode locking and 6.8 mW average power output at the pump power of 160 mW. Figure 2(a) illustrates the optical spectrum of the PM mode-locked fiber oscillator, the spectrum is centered at 1559 nm with the full width at half maximum (FWHM) of 29 nm. The corresponding autocorrelation traces of the mode-locked

signal pulses is shown in Fig. 2(b), the pulse width is equal to 307 fs at the output port of the oscillator, by assuming a sech^2-function pulse profile. The repetition rate of the oscillator is approximately 42.7 MHz, as shown in Fig. 2(c), the measured value is consistent with the calculated value based on the oscillator cavity length mentioned above.

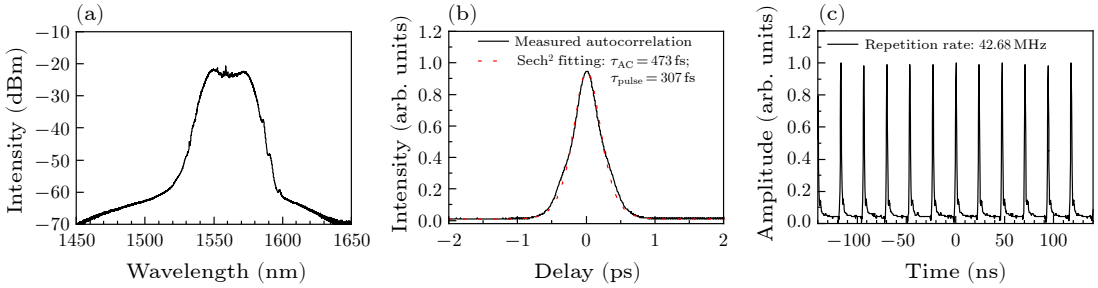

Fig. 2. Temporal and spectral characteristics of oscillator.

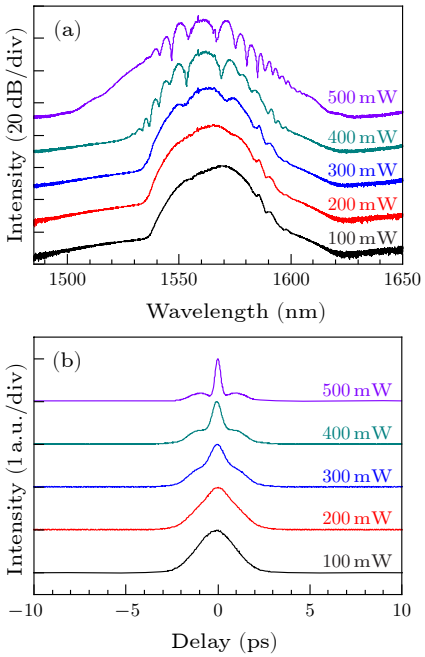

Fig. 3. Temporal and spectral characteristics of pre-amplification stage versus the pump power of pre-amplification stage.

The temporal and spectral characteristics of the output pulses from pre-amplification stage for different pump power are shown in Fig. 3. The spectra have been offset vertically for clarity. The pre-amplification stage utilizes nonlinear compression to achieve ultra-short pulses output. With increase of the pump power, the output optical spectrum of the pre-amplification stage is modulated by the nonlinear effects generated in the amplifier. The corresponding pulse width is compressed under the combined effect of self-phase modulation and the anomalous dispersion. As the pump power is increased to 500 mW, the signal pulse width has been compressed to 240 fs assuming Gaussian pulse profile. However, the output pulse of the pre-amplification stage is used as the signal light of the main amplifier, which needs to avoid strong nonlinear modulation. Considering the pigtail length of the isolator (ISO) placed between the pre-amplification stage and the main amplifier, the pump power of pre-amplification stage is controlled at 270 mW, corresponding average output power of 44 mW. The measured result of optical spectrum and autocorrelation trace after pre-amplification stage are depicted in Fig. 4. Because of the gain narrowing, the FWHM of the signal pulse spectrum after pre-amplification stage is decreased to 9.4 nm, and the corresponding pulse width is calculated to approximately 1.04 ps assuming Gaussian pulse profile. The pulse has uncompensated chirp, which could be further compressed within the passive fiber of the ISO and a short length of the PM erbium/ytterbium-doped fiber.

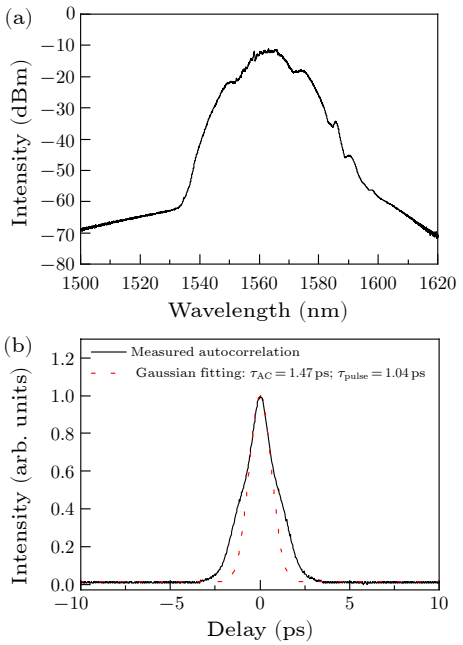

Fig. 4. Temporal and spectral characteristics of pre-amplification stage at the pump power of 270 mW.

The output characteristics of the main amplifier versus the pump power of the main amplifier are evident in Fig. 5. The spectral characteristics of output pulses from main amplifier measured with a spectral resolution of 1 nm by employing a Zolix Omni-λ3015i grating spectrometer. As stated above, the main amplifier is designed to boost the signal power and to realize Raman-induced SSFS. As the pump power is continuously increased, the average power

of the fundamental signal pulse at 1.56 μm increases, providing the energy for Raman solitons to shift to longer wavelengths. Within the pump power range of 13–18 W, tunable Raman soliton outputs can be obtained in the wavelength range of 1685–1711 nm, as shown in Fig. 5(b). The spectra have been offset vertically for clarity. The output power of Raman solitons versus the pump power of the main amplifier is depicted in Fig. 5(c). The power of Raman soliton is a value calculated by the soliton energy proportion of the total energy (based on integrating of the area under the measured spectral curve). By analysis in combination with Fig. 5(a), it can be known that the average power of Raman solitons shows an overall downward trend with increasing pump power. The reason for this phenomenon is that the SSFS process of our laser system is generated in the amplifier fiber, the increasing effective interaction length with the increase of pump power leads to decrease in soliton energy at high pump power.[19] At the 16 W pump power of main amplifier, the Raman soliton at the central wavelength of 1702 nm with FWHM of 20.6 nm is obtained, corresponding average output power of 283 mW.

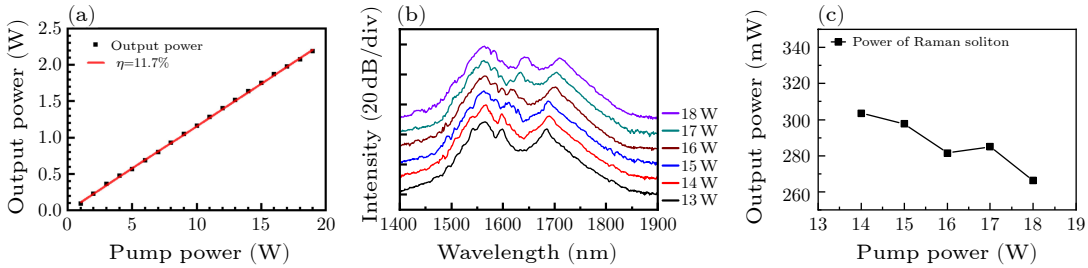

Fig. 5. (a) Output power and (b) optical spectrum versus the pump power of the main amplifier, (c) calculated power of Raman soliton versus the pump power of the main amplifier.

Considering that the structure of the main amplifier is backward pumped, to further support the viewpoint that the Raman soliton is generated in an active fiber of the main amplifier, we added a 4-m-long passive fiber (Nufern PM-GDF-1550) after the experimental setup in Fig. 1. The experimental result is shown in Fig. 6, the spectral characteristics were obtained by using Thorlabs OSA205C Fourier transform optical spectrum analyzers. Compared to the result without adding passive optical fiber, the central wavelength of the Raman soliton output of the system remains unchanged under the condition of ensuring the same pump power of all amplifiers in the system.

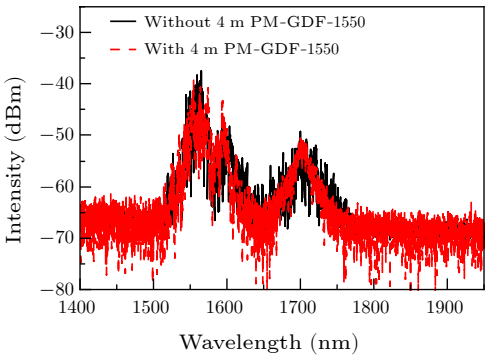

Fig. 6. Measured output spectrum of the main amplifier with (red dot) and without (black line) 4-m-long passive fiber.

The autocorrelation trace of the main amplifier output pulse at the pump power of 16 W is shown in Fig. 7. The temporal characteristics of the system were measured by the using an FR-103 XL autocorrelator. The duration is 515 fs by assuming a Gaussian pulse profile, which is wider than the Fourier transform limit pulse width (approximately 207 fs) corresponding to the spectrum. The larger width of soliton pulse might be caused by the dispersion provided by the combiner fiber pigtail, which can be further compressed by optimizing the pigtail length of the combiner.

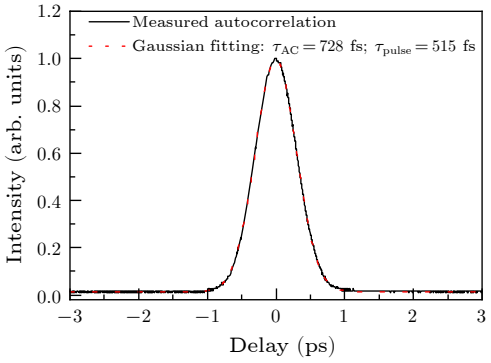

Fig. 7. Measured autocorrelation trace of Raman soliton at the pump power of 16 W.

In conclusion, high-power Raman solitons working at 1.7 μm are directly generated in an all-fiber PM erbium-doped amplifier. By optimizing the ultra-short pulse based on nonlinear compression generated from pre-amplification stage, our system consisting of commercial silica fibers and devices realizes Raman-induced SSFS in main amplifier, which can deliver 42.7 MHz, 283 mW, 515 fs Raman solitons at 1702 nm wavelength. The entirely fiberized alignment-free design of the PM laser system increases the suitability of soliton generation. Our experiment provides a feasible method for high-power all-fiber polarization maintaining femtosecond laser generation working at 1.7 μm.

Acknowledgments. Supported by the National Natural Science Foundation of China (Grant Nos. 10225417 and 61675009), the Natural Science Foundation of Beijing

Municipality (Grant Nos. 4204091 and KZ201910005006), and the China Postdoctoral Science Foundation (Grant No. 212423).

References

[1] Alzeeb G, Dubreuil M, Arzur D *et al.* 2022 *Biomed. Opt. Express* **13** 3120
[2] Lee M, Kannan S, Muniraj G *et al.* 2022 *Tissue Eng. Part B-Rev.* **28** 926
[3] Xiao Y J, Deng P, Zhao Y G *et al.* 2023 *Front. Neurosci.-SWITZ* **17** 1085682
[4] Qin M Y *et al.* 2023 *J. Biophoton.* **16** e202200365
[5] Guo Y, Wang L W, Luo Z Y *et al.* 2023 *Molecules* **28** 4936
[6] Benkowska-Biernacka D, Mucha S G, Firlej L *et al.* 2023 *ACS Appl. Mater. Interfaces* **15** 32717
[7] Li L H, Huang X X, Zhang S C *et al.* 2023 *BMC Cancer* **23** 38
[8] Wang K, Pan Y, Tong S *et al.* 2021 *Biomed. Opt. Express* **12** 6474
[9] Chen J X, Zhan Z Y, Li C *et al.* 2021 *Opt. Lett.* **46** 5922
[10] Wang K, Horton N G, Charan K, and Xu C 2014 *IEEE J. Sel. Top. Quantum Electron.* **20** 6800311
[11] Li B, Wang M R, Charan K *et al.* 2018 *Opt. Express* **26** 19637
[12] Gan M Y, He C, Liu H J *et al.* 2019 *J. Biophoton.* **12** e201900069
[13] Cheng H, Zhong J C, Qiu P, and Wang K 2024 *J. Innov. Opt. Heal. Sci.* **17** 2350011
[14] Anashkina E A, Andrianov A V, Koptev M Y *et al.* 2012 *Opt. Express* **20** 27102
[15] Ruan Q J *et al.* 2017 *IEEE Photon. J.* **9** 7100807
[16] Fang X, Wang Z Q, and Zhan L 2017 *Opt. Eng.* **56** 046107
[17] Stachowiak D, Marzejon M, Bogusławski J *et al.* 2022 *Biomed. Opt. Express* **13** 1899
[18] He X, Lin Q M, Guo H Y *et al.* 2019 *Appl. Phys. Express* **12** 072007
[19] Nicholson J W, Desantolo A, Kaenders W, and Zach A 2016 *Opt. Express* **24** 23396
[20] Nicholson J W, Ahmad R, DeSantolo A, and Várallyay Z 2017 *J. Opt. Soc. Am. B* **34** A1
[21] Hekmat M J, Omoomi M, Gholami A *et al.* 2018 *Appl. Phys. B* **124** 4
[22] Chen X W, Lin W, Wang W L *et al.* 2021 *Opt. Lett.* **46** 1872
[23] Wang M X, Li P X, Xu Y T *et al.* 2022 *Chin. Phys. Lett.* **39** 024201